Significant Enhancement of Single-Walled Carbon Nanotube Based Infrared Photodetector Using PbS Quantum Dots

Yicheng Tang, Hehai Fang, Mingsheng Long, Gang Chen, Zhe Zheng, Jin Zhang, Wenjia Zhou, Zhijun Ning, Zhihong Zhu, Ying Feng, Shiqiao Qin, Xiaoshuang Chen, Wei Lu, and Weida Hu, *Member, IEEE*

(Invited Paper)

***Abstract*—We show that the performance of single-walled carbon nanotubes (SWCNTs) based infrared photodetector can be greatly enhanced through the combination with colloidal PbS quantum dots (QDs). To improve the photo-induced charge transport efficiency and the carrier mobility, the colloidal PbS QDs are modified by short-chain inorganic. Under illumination, the light-induced electron-hole pairs can be effectively separated by the internal electric field formed at the interfaces between SWCNTS and PbS QDs, which will lead to the increase of both conductivities in them. Photocurrent is formed under the driving of source-drain voltage ($V_{\rm ds}$) applied by the interdigital finger electrodes. Our hybrid phototransistor achieves a responsivity of 7.2 A/W, a specific detectivity (defined below) of 7.1×10^{10} Jones, and a response time of 1.58 ms at the same time under 1550-nm illumination with low intensity. Through gate voltage tuning, the responsivity can be increased to 353.4 A/W. In addition, our hybrid phototransistor is stable, low-cost, and compatible with complementary metal oxide semiconductor, which benefits a lot in real applications.**

***Index Terms*—Carbon nanotubes, infrared photodetector, photogating effect, quantum dots.**

Manuscript received January 10, 2018; revised March 12, 2018; accepted March 22, 2018. Date of publication March 29, 2018; date of current version April 17, 2018. This work was supported in part by the National Natural Science Foundation of China under Grants 11734016, 61674157, 61521005, and 61725505; and in part by the Key Research Project of Frontier Sciences of CAS under Grant QYZDB-SSWJSC031. *(Corresponding author: Weida Hu.)*

Y. Tang is with the State Key Laboratory of Infrared Physics, Shanghai Institute of Technical Physics, Chinese Academy of Sciences, Shanghai 200083, China, and also with the College of Optoelectronic Science and Engineering, National University of Defense Technology, Changsha 410073, China.

H. Fang, M. Long, G. Chen, X. Chen, W. Lu, and W. Hu are with the State Key Laboratory of Infrared Physics, Shanghai Institute of Technical Physics, Chinese Academy of Sciences, Shanghai 200083, China (e-mail: wdhu@mail.sitp.ac.cn).

Z. Zheng and J. Zhang are with the State Key Laboratory for Structural Chemistry of Unstable and Stable Species, College of Chemistry and Molecular Engineering, Peking University, Beijing 100871, China.

W. Zhou and Z. Ning are with the Key Laboratory of Infrared Imaging Materials and Detectors, Shanghai Institute of Technical Physics, Chinese Academy of Sciences, Shanghai 200083, China.

Z. Zhu, Y. Feng, and S. Qin are with the College of Optoelectronic Science and Engineering, National University of Defense Technology, Changsha 410073, China.

Color versions of one or more of the figures in this paper are available online at http://ieeexplore.ieee.org.

Digital Object Identifier 10.1109/JSTQE.2018.2819904

I. Introduction

IN VARIOUS demanding applications, such as telecommunication, thermal imaging, biological imaging, and remote sensing, infrared (IR) photodetectors play a key role [1]–[3]. The high performance 1.55 μm photodetector is especially desired for the optical communication system and imaging system because of the low optical attenuation at this wavelength [4]. Most commercial infrared detectors are based on semiconductors like HgCdTe, InSb, and InGaAs. However, high cost of material growth and extra cooling requirements limit their applications. Recently, room-temperature IR photodetectors based on quantum dots (QDs) [5]–[7], graphene [8], [9], black phosphorus [10], black arsenic phosphorus [11], and carbon nanotubes [12]–[14] have been extensively studied. In addition, the hybrid IR photodetectors based on two or more different materials exhibit excellent performance, such as MoS_2-graphene-WSe_2 van der waals heterostructure for broadband photodetection [15], GaSe-GaSb vertical heterostructure for Dual-band detection [16], and graphene/PbS quantum dots nanohybrids for near-infrared detection [17]. Carbon nanotubes (CNTs), depending on the arrangement of the carbon-atom honeycomb structure with respect to their axis, can be divided into direct band semiconductors (sc-CNTs) and metals with nearly ballistic conduction [18]. Depending on the curved wall number, they also can be divided into single-walled carbon nanotubes (SWCNTs) and multi-walled carbon nanotubes (MWCNTs). Studies show that semiconducting single-walled carbon nanotubes (sc-SWCNTs) are promising building blocks for fabricating high-performance IR photodetector because of their ultrafast charge transport mobility, compatible band gaps, excellent electronic properties and great mechanical and chemical stabilities [12], [18]. In addition, sc-SWCNT film based photoconductors show compatibility with complementary metal oxide semiconductor (CMOS) fabrication processing, potentially enabling on-chip integrated, and multifunctional optoelectronics [19].

However, due to the enhanced Coulomb interaction and the reduced screen effect in one-dimensional materials, the photon-generated excitons are strongly bonded in CNTs and thus lead to only a small fraction of electron-hole pairs that can be separated to form effective photocurrent [18], [20], [21]. These properties generally render CNTs based photodetectors

bolometric in nature, wherein the excitons recombine non-radiatively and transfer its energy to the crystal lattice of CNTs [22], [23]. As a result, the performance of CNTs film based IR photodetectors could not be comparable to IR photodetectors comprised of other nanostructured materials [17], [24], [25].

Recently, CNTs based hybrid photodetectors show significant improvements in photosensitivity. Highly sensitive photodetectors realized by graphene-CNTs film [26] and MoS_2-CNTs [27] heterojunction have been reported. Nevertheless, these devices are hard to fabricate and difficult to form detecting arrays which are disadvantages in real applications. With the merits of facile solution processability, low-cost manufacturing and tunable bandgap [1], colloidal QDs become the promising candidate for next-generation IR detection. Due to the high light absorption and long lifetime of carriers in QDs, the quantum efficiency of a QDs based IR photoconductor can be as high as 10^3 [28]. However, the devices composed of single-layer QDs still suffer from the drawbacks of large dark currents, low on-off ratios and slow photoresponse speed which are prevailing problems in photoconductive devices and can be the obstacles in real applications [29], [30]. To pursue high performance IR photodetectors along with the merits of CMOS compatible, on-chip integratable and easy to be fabricated, colloidal QDs and CNTs, one of the most potential combination, have been investigated [19], [31]–[34]. The colloidal QDs, most used as light absorber in these hybrid structures, trap one type of light-induced carriers and inject the other type to the CNTs which acts as channel, thus results the change of channel conductivity. This photo-response mechanism is named photogating effect [19], [33]–[35]. Although improvements have been shown in these works, the detectivities, response time and dark current of these hybrid photodetectors still cannot meet the requirement of real applications. Important reasons for this are the low charge transport efficiency between QDs and CNTs and the low carrier mobility in QDs [33], [34].

Here we demonstrate a novel SWCNTs-based phototransistor utilizing colloidal PbS QDs as both photogating layer and light absorbing layer. To improve the photo-induced charge transport efficiency and the carrier mobility of PbS QDs, we use short-chain inorganic ligands tetrabutylammoniumiodide (TBAI) instead of the traditional long-chain organic ones to modify PbS QDs [7], [36]. Furthermore, the ligand treatment can also tune the energy levels of PbS QDs by forming different dipole moments at the QD–ligand interface [7]. Thus, electron-donating ligand TBAI can shift the valance band to lower energy and thus to form n-type PbS QDs [36]. When the n-type PbS QDs contact with p-type SWCNTs, a built-in electric field formed at the interface (like PN junction) between SWCNTs and PbS QDs can effectively separate the light-induced electron-hole (e-h) pairs, drawing electrons into PbS QDs and holes into SWNCTs respectively. Under the drive of source-drain voltage (V_{ds}), these light-induced charges are transported in opposite direction and collected by the electrodes, which results the photocurrent.

II. Results and Discussion

The three-dimensional schematic of the device is depicted in Fig. 1(a). A film with highly enriched SWCNTs is formed through the deposition of SWCNTs solution on the substrate (SiO_2/Si). Au interdigital finger electrodes with Pd adhesion layers (each 4 μm in period and 600 nm in width) are used to ensure good contact with SWCNTs. PbS QDs are spin-coated onto the structure with detailed information in the Methods Section. Since the PbS QDs layer is not isolated with the electrodes, electron-hole pairs generated near the electrode region (dash square in Fig. 1(b)) could recombine before collected by the external circuit, and do not contribute to the photocurrent. However, for photogenerated e-h pairs in the middle-channel region, they can be fast-separated by the built-in field between QDs and SWCNTs and transport in opposite direction driven by the external bias voltage. This significantly contributes to the photoconductance, as some reported devices with similar structure [17], [19]. Therefore, we ignore the unpassivation of the electrodes here.

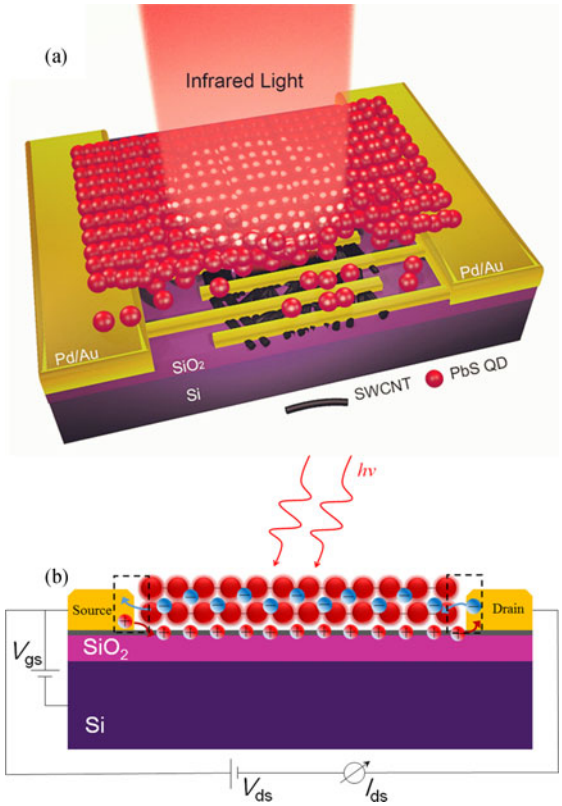

Fig. 1. (a) Three-dimensional schematic of the SWCNT film-PbS QDs hybrid phototransistor with interdigital finger electrodes. (b) Schematic of the photo-response circuit of the device showing the voltage bias. V_{ds}, source–drain voltage; V_{gs}, gate–source voltage.

To further clarify the response mechanism, the band diagram for charge transfer between the SWCNTs and TBAI-processed PbS QDs under illumination is depicted in Fig. 2(a) [7], [37]. When the n-type PbS QDs contact p-type SWCNTs, due to the free diffusion and recombination of major carriers (electrons in PbS QDs and holes in SWCNTs), a depletion region will form at the interface, resulting in the band bending like common PN junctions. With the assist of built-in electric field, light-induced electron-hole pairs can be effectively separated, and the electrons are transferred into PbS QDs whereas the holes are transferred into SWCNTs.

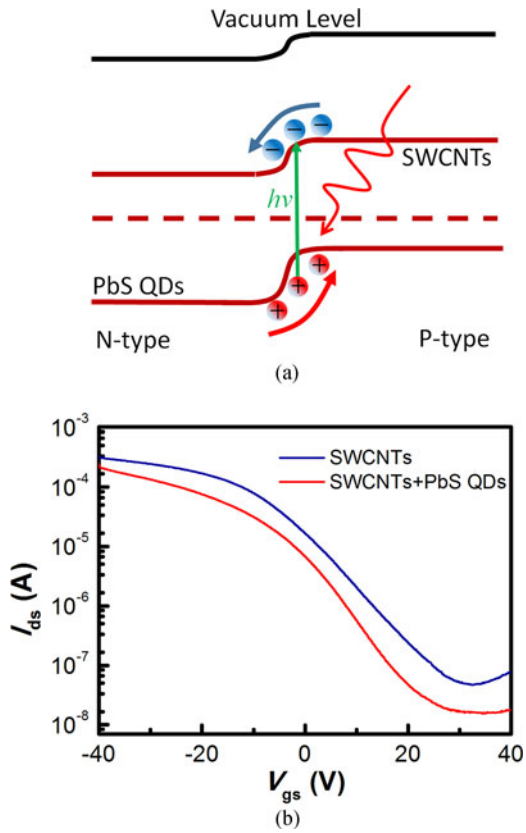

Fig. 2. (a) Schematic of band diagram for built-in electric field assisted charge transfer between PbS QDs and SWCNTs under illumination. (b) Transfer characteristics of SWCNTs film only and PbS QDs/ SWCNTs hybrid structure with $V_{ds} = 1$ V.

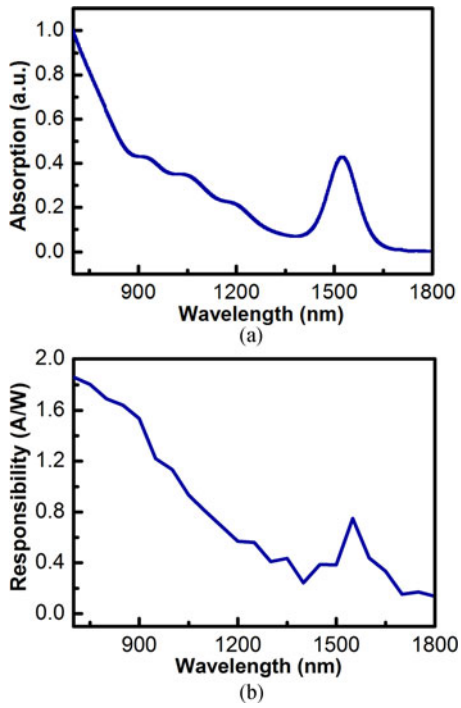

Fig. 3. (a) Normalized absorption spectra of the PbS QDs. (b) Normalized spectral responsivity of the hybrid phototransitor with $V_{gs} = 30$ V and $V_{ds} = 1$ V.

To verify the strong interaction between SWCNTs and PbS QDs, we measured the transfer characteristics of the same SWCNTs film before and after spin-coating of PbS QDs as shown in Fig. 2(b). In the transfer characteristics of SWCNTs film, the blue solid curve in Fig. 2(b), the back-gate tunable on/off ratio of 10^4 shows the great semiconductor property of the SWCNTs film and verifies that our SWCNTs film is mostly composed of sc-SWCNTs. Comparing the transfer characteristics of the same SWCNTs film before (blue curve) and after spin-coating PbS QDs (red curve), we found that the I_{ds} of the spin-coated hybrid structure is smaller. On one hand, this phenomenon can be due to the strong doping effect. Because of the different electron densities in PbS QDs and SWCNTs, electrons in n-type QDs will freely diffuse to the p-type SWCNTs and lower the free carrier concentration in SWCNTs. On the other hand, the defects induced by QDs may slightly lower the carrier mobility in SWCNTs. And because QDs layer has a very low electron mobility, the main conductance of the device is from the SWCNTs. Thus the dark current after spin coating is smaller, represented by the decreasing of I_{ds}. At the same time, the free electrons or holes diffusion in this hybrid structure leads to the band bending as depicted in Fig. 2(a), results the built-in electric field which assists the separation of light-induced e-h pairs.

As mentioned above, the PbS QDs film works as the light absorption layer in our hybrid structure. To verify our design, we have measured the absorption spectra of the pure PbS QDs and the spectral responsivity of the hybrid phototransistor. Results are demonstrated in Fig. 3. In Fig. 3(a), an obvious absorption peak at 1550 nm is clearly shown. This can be attributed to the particular size of the PbS QDs which affects the band structure [1]. After the PbS QDs are spin-coated on the SWCNTs, the normalized spectral responsivity of this hybrid structure still shows a similar shape with rising and down trends like the absorption spectra of pure PbS QDs. Moreover, the 1550 nm peak exists in both the spectral responsivity of the device and the absorption spectra of the PbS QDs. Consequently, it is reasonable to believe that the light absorption of the PbS QDs in the hybrid phototransistor dominates the photoresponse of the whole structure in the IR region.

In Fig. 4(a), we plot the transfer characteristics of SWCNTs-PbS QDs hybrid phototransistor in the dark and under 1550 nm illumination in linear and log-scale at $V_{ds} = 1$ V. In the linear-scale transfer curves, a positive shift in the threshold voltage (V_{TH}) of $\sim$5 V can be observed, which can be attributed to the increase of hole concentration in the SWCNTs [38]. Because the increase of hole concentration brings the Fermi-level closer to the valence band, less negative gate voltage is required to shift down the Fermi-level to the valence band to turn the device on [19]. The increase of hole concentration under illumination can be explained by the separation of light-induced electron-hole pairs and accumulation of holes in the SWCNTs side driven by built-in electric field, which has been discussed in detail in Fig. 2(a). In the log-scale transfer curves, when V_{gs} is larger than 20 V, the device is depleted, so the dark current of the whole hybrid phototransistor dramatically decreases which is beneficial to weak light detection. In addition, the gate tunable ability

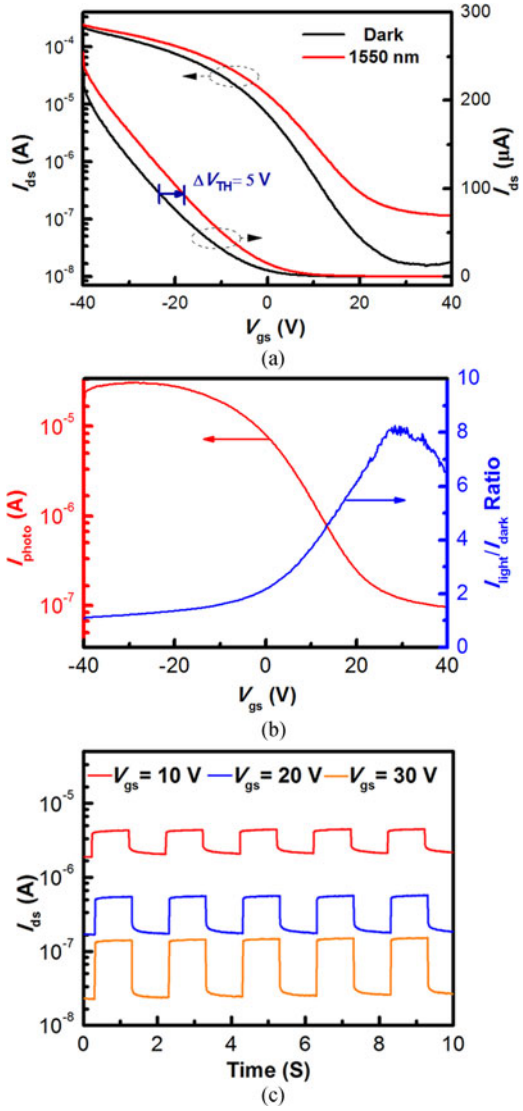

Fig. 4. (a) Transfer characteristics of SWCNTs-PbS QDs hybrid phototransistor in the dark and under 1550 nm illumination in linear and log-scale with $V_{ds} = 1$ V. (b) Photocurrent (I_{photo}) and I_{light}/I_{dark} ratio of the hybrid phototransistor under 1550 nm illumination as a function of back-gated voltages with $V_{ds} = 1$ V. (c) Photoswitching behavior of the hybrid phototransistor under 0.5 Hz 1550 nm illumination with different V_{gs} at $V_{ds} = 1$ V. The light intensities used here are all 28 mW/cm^2.

of our device is shown in Fig. 4(b). The maximum photocurrent 31.1 μA occurs at $V_{gs} = -28$ V, and the calculated responsivity at this condition is 353.4 A/W. Such a high responsivity is due to the high gain originating from the photogating effect in which the photo-induced e-h pairs are respectively separated into the QDs gating layer and the SWCNTs channel by the strong built-in electric field. For weak light detection, I_{light}/I_{dark} ratio is very important. Here, it reaches the maximum of more than 8 at $V_{gs} = 30$ V and $V_{ds} = 1$ V. This tunable feature makes our phototransistor more flexible in various applications.

The stability and photoswitching characteristic of the hybrid phototransistor under 0.5 Hz 1550 nm illumination has been demonstrated in Fig. 4(c) with $V_{gs} = 10, 20, 30$ V and $V_{ds} = 1$ V. The response of our device is stable at all gate bias. It is

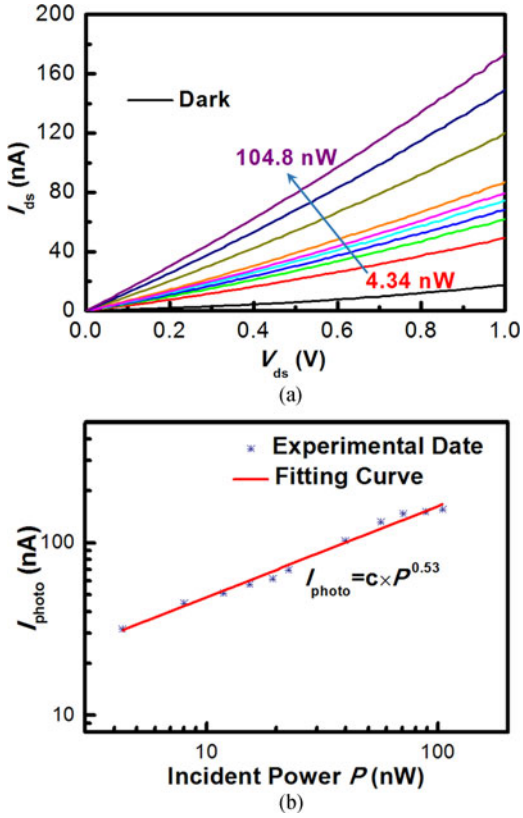

Fig. 5. (a) Liner I_{ds} versus V_{ds} curves under 1550 nm illumination with different illumination power intensities varied from 4.34 nW to 104.8 nW at $V_{ds} = 1$ V and $V_{gs} = 30$ V. (b) Dependence of photocurrent on illumination power intensities.

found that the on–off photoswitching ratio is more significant at $V_{gs} = 30$ V. Taking $V_{gs} = 30$ V and $V_{ds} = 1$ V, our device shows a relative high I_{light}/I_{dark} ratio and an acceptable photocurrent.

The optoelectronic performances of the hybrid phototransistors under different illumination power intensities are depicted in Fig. 5(a). The photocurrent increases gradually when the optical power increases from 4.34 nW to 104.8 nW. Fig. 5(b) directly shows the dependence of photocurrent on various illumination power intensities. The relationship between photocurrent and light intensity obeys the power law $I = cP^k$ [39], where I is the photocurrent, c is a proportionality constant relates to the data units, P is the incident power, and k is an empirical value. Through nonlinear fitting, we can obtain $c = 2.13 \times 10^{-5}$ and $k = 0.53$, depending on the complex processes of electron-hole generation, trapping, and recombination [39].

The responsivity (R) and the specific detectivity (D^*) are also two key parameters for a photodetector and they have been depicted in Fig. 6. The responsivity of a photodetector can be defined as $R = I_{photo}/P$ where I_{photo} is the photocurrent and P is the incident power. Moreover, the specific detectivity is an important figure-of-merit representing the capability of the lowest detectable signal for a photodetector, which can be defined as $D^* = (A\Delta f)^{1/2}/(\text{NEP})$, where A is the effective area of the detector calculated as 3×10^{-6} cm^2 in Methods Section, Δf is the electrical bandwidth in Hz, and NEP is the noise equivalent power. Considering the shot noise from dark

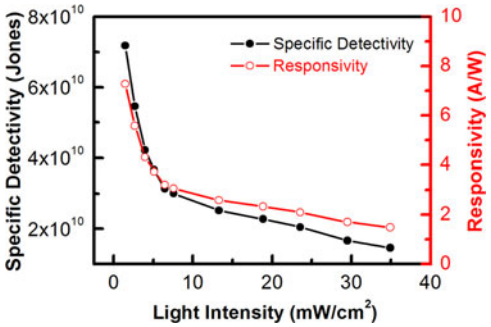

Fig. 6. Specific detectivity and responsivity of the hybrid phototransistor at $V_{ds} = 1$ V and $V_{gs} = 30$ V.

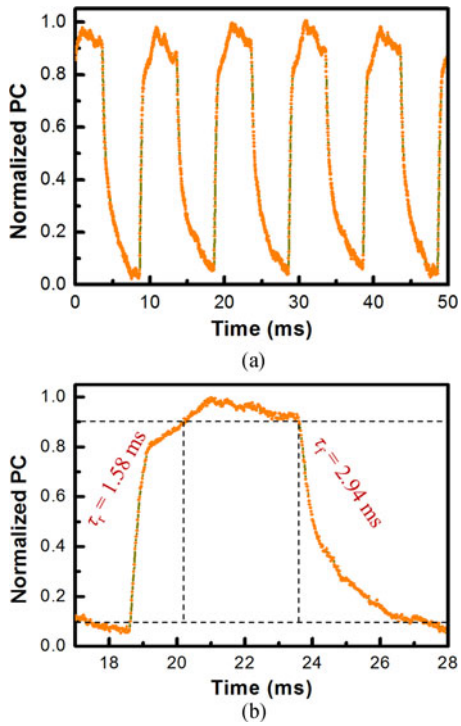

Fig. 7. (a) Normalized photocurrent versus time under 100 Hz 1550 nm illumination at $V_{gs} = 30$ V and $V_{ds} = 1$ V. (b) The enlarged picture to show detailed rise time (τ_r) and fall time (τ_f) of the hybrid phototransistor.

current is the major factor limiting the detectivity, the specific detectivity can be expressed as $D^* = RA^{1/2}/(2eI_{dark})^{1/2}$ [38], [40], where R is the responsivity, e is the electronic charge, and I_{dark} is the dark current. Under low light intensity, the D^* and R of the hybrid phototransistor are up to 7.1×10^{10} Jones and 7.2 A/W. Nevertheless, the D^* and R decreases with the increase of incident light intensity which is due to the saturation effect and is also common in other IR photoconductors based on PbS QDs [28]. Note that these parameters can be further improved through changing V_{gs}, at the cost of the decreasing in I_{light}/I_{dark} ratio, which has already been discussed above in Fig. 4(b).

As a photodetector, response time is another important parameter which can dramatically affect the application prospects. Fig. 7(a) shows the normalized photocurrent of the hybrid phototransistor with $V_{gs} = 30$ V and $V_{ds} = 1$ V under 100 Hz 1550 nm illumination. The response of our device is stable and can follow

TABLE I
COMPARISON OF THE CRITICAL PARAMETERS FOR ROOM-TEMPERATURE CNT-BASED PLANAR PHOTODETECTOR

R (AW^{-1})	D* ($cmHz^{1/2}W^{-1}$)	Response time	Wavelength	Reference
-	3.3×10^6	1-2 ms	IR radiation	[41]
0.048	6×10^{11}	-	1205 nm	[42]
-	1.22×10^8	0.94 ms	1800nm	[43]
0.016	2.3×10^8	1 ms	1050 nm	[37]
9.87×10^{-5}	1.09×10^7	-	785 nm	[12]
-	1.5×10^7	1.5 ms	NIR	[44]
-	4×10^6	800 ms	940 nm	[45]
97.5	1.17×10^9	1.7 ms	1200 nm	[19]
353.4	7.1×10^{10}	1.58 ms	1550 nm	This work

the original 100 Hz IR signal, which proves the bright application prospects of our device in IR detecting and IR imaging. The detailed rising time $\tau_r = 1.58$ ms (defined as 10% to 90%) and falling time $\tau_f = 2.94$ ms (defined as 90% to 10%) are demonstrated in Fig. 7(b). The short rising time of our device under illumination originates from the built-in electric fields at the interfaces between SWCNTS and PbS QDs which greatly accelerates the separation of photo-induced e-h pairs. The falling time, compared to the rising time, is slightly longer. The defects in the device that can catch the photo-induced electrons and holes and prevent their recombination may account for this.

In this section, we have discussed the working mechanism and the key parameters of our photodetector, R of 353.4 A/W, D^* of 7.1×10^{10} Jones and τ_r of 1.58 ms can be achieved under 1550 nm illumination. Table I lists the critical parameters of other reported CNT-based photodetectors. Compared to them, our device shows significant enhancements.

III. METHODS

A. Device Fabrication

The SWCNTs have been separated by polymer-assisted sonication mentioned in previous work and the extra polymers are removed by filtration [46]. Then, the substrate Si with 300nm SiO_2 is dip-coated in the SWCNTs solution for 4 h at 60 °C. In order to clean the surface of substrate, the tetrahydrofuran is used to wash out the residue of solvent and impurity followed by baking at 200 °C. After that, we drop SWCNTs solution 20 times on the substrate with the operation of clean carried out every fifth time. Thus to produce a SWCNTs film about 10 nm in thickness and 120 nanotubes per μm^2 in density. Finally, the sample is annealed in the chemical vapor deposition oven for 2 h at 400 °C under the protection of 300 standard-state cubic centimeter per minute (sccm) Argon and 100 sccm hydrogen.

The interdigital finger electrodes on the SWCNTs is defined through electron-beam lithography process followed by the thermal evaporation of 3nm Pd and 50 nm Au. We use high-work function metal Pd as adhesion layer here to promise ohmic contacts with SWCNTs. Then the SWCNTs film is isolated through oxygen ion etching. The dark dotted box in Fig. 8(a) shows the etched SWCNTs film with the size of 30 μm in length and 12 μm in width. Taking consideration of the size and distribution of interdigital finger electrodes

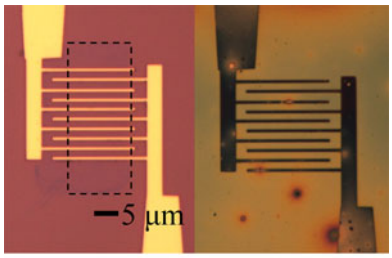

Fig. 8. (a) Optical image of the etched SWCNTs film with interdigital finger electrodes, where the dark dotted box shows the film edges. (b) Optical image of the device after the LBL spin-coating process of PbS QDs.

simultaneously, we can conservatively regard the effective response area A of our device as 300 μm^2. The colloidal PbS QDs film is built through layer-by-layer (LBL) approach under ambient atmosphere. Briefly, PbS QDs solution (50 mg ml^{-1}) are put on the SWCNTs film and spin-coated at 2500 rpm for 30 s, then the TBAI solution was put on the formed PbS QDs layer for 30 s to complete the ligand exchange, followed by two rinse-spin steps with methanol. These processes are repeated three times to get a PbS QDs film with about 80nm in thickness [7]. Fig. 8(b) demonstrates the optical picture of the device after the LBL spin-coating process of PbS QDs and which shows the uniform distribution of PbS QDs in the channels.

B. Characterization

The electrical characterizations are recorded by a Keysight B1500 semiconductor characterization system combined with a Lake Shore TTPX Probe Station under vacuum at room temperature. The 1550 nm illumination is applied by a Single Mode Laser Diode to perform the optoelectronic characterization. The response time of the device is measured by the Tektronix Oscilloscope MDO3014 with a pre-amplifier. For the responsivity versus wavelength plot, a wide-spectrum laser source, a monochrometer and optical attenuation devices are employed to produce the light source from 700 nm to 1800 nm with the same intensity of 141.47 mW/cm^2.

IV. Conclusion

Here, we have demonstrated a hybrid SWCNTs/PbS QDs phototransistor. The strong junction formed by n-type photogating layer TBAI modified PbS QDs and p-type channel SWCNTs enables the efficient separation of photo-induced e-h pairs, thus high gain and fast response are realized in our device. The responsivity of up to 353.4 A/W, the specific detectivity of 7.1 $\times$ 10^{10} Jones, and a response time of 1.58 ms have been achieved, showing the potential of SWCNTs in the infrared optoelectronic applications. To further enhance the performance, densely aligned SWCNTs are desired since through which the IR absorption and the mobility of carriers can be maximized [47]. Using asymmetrical electrode, such as Pd and Sc, to form suitable Schottky junction is also a helpful method. Last but not least, QD is one of the most promising materials to effectively enhance the SWCNTs-based infrared detector, so other QDs to further optimize the heterojunction with SWCNTs and the better ligand which can further improve the photo-induced charge transport efficiency between them are all important aspects to do research.

References

[1] G. Konstantatos and E. H. Sargent, "Nanostructured materials for photon detection," *Nature Nanotechnol.*, vol. 5, pp. 391–400, Jun. 2010.
[2] F. P. G. D. Arquer, A. Armin, P. Meredith, and E. H. Sargent, "Corrigendum: Solution-processed semiconductors for next-generation photodetectors," *Nature Rev. Mater.*, vol. 2, Mar. 2017, Art. no. 17012.
[3] R. Saran and R. J. Curry, "Lead sulphide nanocrystal photodetector technologies," *Nature Photon.*, vol. 10, pp. 81–92, Jan. 2016.
[4] X. G. Meng *et al.*, "Near infrared broadband emission of bismuth-doped aluminophosphate glass," *Opt. Express*, vol. 13, pp. 1628–34, Mar. 2005.
[5] G. Konstantatos and E. H. Sargent, "Colloidal quantum dot photodetectors," *Infrared Phys. Technol.*, vol. 54, pp. 278–282, May 2011.
[6] N. Huo, S. Gupta, and G. Konstantatos, "MoS_2-HgTe quantum dot hybrid photodetectors beyond 2 μm," *Adv. Mater.*, vol. 29, May 2017, Art. no. 1606576.
[7] Z. Ren *et al.*, "Bilayer PbS quantum dots for high-performance photodetectors," *Adv. Mater.*, vol. 29, Sep. 2017, Art. no. 1702055.
[8] B. Chitara, L. S. Panchakarla, S. B. Krupanidhi, and C. N. Rao, "Infrared photodetectors based on reduced graphene oxide and graphene nanoribbons," *Adv. Mater.*, vol. 23, pp. 5419–5424, Jul. 2011.
[9] N. Guo *et al.*, "High-quality infrared imaging with graphene photodetectors at room temperature," *Nanoscale*, vol. 8, pp. 16065–16072, Sep. 2016.
[10] L. Ye *et al.*, "Highly polarization sensitive infrared photodetector based on black phosphorus-on-WSe 2 photogate vertical heterostructure," *Nano Energy*, vol. 37, pp. 53–60, 2017.
[11] M. Long *et al.*, "Room temperature high-detectivity mid-infrared photodetectors based on black arsenic phosphorus," *Sci. Adv.*, vol. 3, Jul. 2017, Art. no. e1700589.
[12] J. Liu *et al.*, "Carbon nanotube arrays based high-performance infrared photodetector," *Opt. Mater. Express*, vol. 2, pp. 839–848, Jun. 2012.
[13] P. L. Ong, W. B. Euler, and I. A. Levitsky, "Carbon nanotube-Si diode as a detector of mid-infrared illumination," *Appl. Phys. Lett.*, vol. 96, Jan. 2010, Art. no. 033106.
[14] S. Nanot *et al.*, "Broadband, polarization-sensitive photodetector based on optically-thick films of macroscopically long, dense, and aligned carbon nanotubes," *Sci. Rep.*, vol. 3, Feb. 2013, Art. no. 1335.
[15] M. Long *et al.*, "Broadband photovoltaic detectors based on an atomically thin heterostructure," *Nano Lett.*, vol. 16, pp. 2254–2259, Apr. 2016.
[16] P. Wang *et al.*, "Arrayed Van Der Waals broadband detectors for dual-band detection," *Adv. Mater.*, vol. 29, Apr. 2017, Art. no. 1604439.
[17] G. Konstantatos *et al.*, "Hybrid graphene-quantum dot phototransistors with ultrahigh gain," *Nature Nanotechnol.*, vol. 7, pp. 363–368, May 2012.
[18] P. Avouris, M. Freitag, and V. Perebeinos, "Carbon-nanotube photonics and optoelectronics," *Nature Photon.*, vol. 2, pp. 341–350, Jun. 2008.
[19] S. Park *et al.*, "Significant enhancement of infrared photodetector sensitivity using a semiconducting single-walled carbon nanotube/C60 phototransistor," *Adv. Mater.*, vol. 27, pp. 759–765, Jan. 2015.
[20] M. Freitag, Y. Martin, J. A. Misewich, R. Martel, and P. Avouris, "Photoconductivity of Single Carbon Nanotubes," *Neuroendocrinology*, vol. 101, pp. 35–44, Jun. 2003.
[21] F. Wang, G. Dukovic, L. E. Brus, and T. F. Heinz, "The optical resonances in carbon nanotubes arise from excitons," *Science*, vol. 308, pp. 838–841, May 2005.
[22] M. E. Itkis, F. Borondics, A. Yu, and R. C. Haddon, "Bolometric infrared photoresponse of suspended single-walled carbon nanotube films," *Science*, vol. 312, pp. 413–416, Apr. 2006.
[23] J. John, M. Muthee, M. Yogeesh, S. K. Yngvesson, and K. R. Carter, "Suspended Multiwall Carbon Nanotube-Based Infrared Sensors via Roll-to-Roll Fabrication," *Adv. Opt. Mater.*, vol. 2, pp. 581–587, Mar. 2014.
[24] V. Sukhovatkin, S. Hinds, L. Brzozowski, and E. H. Sargent, "Colloidal quantum-dot photodetectors exploiting multiexciton generation," *Science*, vol. 324, pp. 1542–1544, Jun. 2009.
[25] X. Gong *et al.*, "High-detectivity polymer photodetectors with spectral response from 300 nm to 1450 nm," *Science*, vol. 325, pp. 1665–1667, Sep. 2009.
[26] T. F. Zhang *et al.*, "Broadband photodetector based on carbon nanotube thin film/single layer graphene Schottky junction," *Sci. Rep.*, vol. 6, Dec. 2016, Art. no. 38569.

[27] D. Jariwala *et al.*, "Gate-tunable carbon nanotube-MoS_2 heterojunction p-n diode," in *Proc. Nat. Acad. Sci. USA*, Nov. 2013, vol. 110, pp. 18076–18080.
[28] G. Konstantatos *et al.*, "Ultrasensitive solution-cast quantum dot photodetectors," *Nature*, vol. 442, pp. 180–183, Jul. 2006.
[29] I. A. De, C. Venettacci, L. Colace, L. Scopa, and S. Foglia, "PbS colloidal quantum dot photodetectors operating in the near infrared," *Sci. Rep.*, vol. 6, Nov. 2016, Art. no. 37913.
[30] C. Hu, A. Gassenq, Y. Justo, and K. Devloo-Casier, "Air-stable short-wave infrared PbS colloidal quantum dot photoconductors passivated with Al_2O_3 atomic layer deposition," *Appl. Phys. Lett.*, vol. 105, pp. 218–220, Oct. 2014.
[31] S. Shukla *et al.*, "Polymeric nanocomposites involving a physical blend of IR sensitive quantum dots and carbon nanotubes for photodetection," *J. Phys. Chem. C*, vol. 114, pp. 3180–3184, Feb. 2010.
[32] S. Jeong, H. C. Shim, S. Kim, and C. S. Han, "Efficient electron transfer in functional assemblies of pyridine-modified NQDs on SWNTs," *ACS Nano*, vol. 4, pp. 324–330, Dec. 2010.
[33] D. Wang *et al.*, "Controlled fabrication of PbS Quantum-Dot/Carbon-Nanotube nanoarchitecture and its significant contribution to Near-Infrared Photon-to-Current conversion," *Adv. Functional Mater.*, vol. 21, pp. 4010–4018, Sep. 2011.
[34] H. C. Shim, S. Jeong, and C. S. Han, "Controlled assembly of CdSe/MWNT hybrid material and its fast photoresponse with wavelength selectivity," *Nanotechnology*, vol. 22, Mar. 2011, Art. no. 165201.
[35] H. Fang and W. Hu, "Photogating in low dimensional photodetectors," *Adv. Sci.*, vol. 4, Oct. 2017, Art. no. 1700323.
[36] R. D. Harris *et al.*, "Electronic processes within quantum dot-molecule complexes," *Chem. Rev.*, vol. 116, pp. 12865–12919, Aug. 2016.
[37] R. Lu, C. Christianson, A. Kirkeminde, S. Ren, and J. Wu, "Extraordinary photocurrent harvesting at Type-II Heterojunction interfaces: Toward high detectivity carbon nanotube infrared detectors," *Nano Lett.*, vol. 12, pp. 6244–6249, Nov. 2012.
[38] S. Heinze *et al.*, "Carbon nanotubes as schottky barrier transistors," *Phys. Rev. Lett.*, vol. 89, Aug. 2002, Art. no. 106801.
[39] N. Guo *et al.*, "Anomalous and highly efficient InAs nanowire phototransistors based on majority carrier transport at room temperature," *Adv. Mater.*, vol. 26, pp. 8203–8209, Dec. 2014.
[40] X. Wang *et al.*, "Ultrasensitive and broadband MoS_2 photodetector driven by ferroelectrics," *Adv. Mater.*, vol. 27, pp. 6575–6581, Nov. 2015.
[41] R. Lu, J. J. Shi, F. J. Baca, and J. Z. Wu, "High performance multiwall carbon nanotube bolometers," *J. Appl. Phys.*, vol. 108, 2010, Art. no. 084305.
[42] D. J. Bindl, M. Y. Wu, F. C. Prehn, and M. S. Arnold, "Efficiently harvesting excitons from electronic type-controlled semiconducting carbon nanotube films," *Nano Lett.*, vol. 11, pp. 455–460, Feb. 2011.
[43] G. Verareveles *et al.*, "High-sensitivity bolometers from self-oriented single-walled carbon nanotube composites," *ACS Appl. Mater. Interfaces*, vol. 3, pp. 3200–3204, Jul. 2011.
[44] R. Lu, C. Christianson, B. Weintrub, and J. Z. Wu, "High photoresponse in hybrid graphene-carbon nanotube infrared detectors," *ACS Appl. Mater. Interfaces*, vol. 5, pp. 11703–11707, Nov. 2013.
[45] J. John, M. Muthee, M. Yogeesh, S. K. Yngvesson, and K. R. Carter, "Suspended multiwall carbon Nanotube-Based infrared sensors via Roll-to-Roll fabrication," *Adv. Opt. Mater.*, vol. 2, pp. 581–587, Feb. 2014.
[46] J. Gu *et al.*, "Solution-processable high-purity semiconducting SWCNTs for large-area fabrication of high-performance thin-film transistors," *Small*, vol. 12, pp. 4993–4999, Sep. 2016.
[47] S. Park, M. Vosguerichian, and Z. Bao, "A review of fabrication and applications of carbon nanotube film-based flexible electronics," *Nanoscale*, vol. 5, pp. 1727–1752, Jan. 2013.

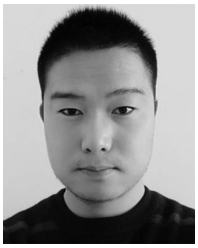

Yicheng Tang received the M.S. degree in optical engineering, in 2016, from the National University of Defense Technology, Changsha, China, where he is currently working toward the Ph.D. degree.

His current research interests include fabrication and characterization of infrared photodetectors based on low-dimensional materials, including quantum Dots, carbon nanotubes, and two-dimensional materials.

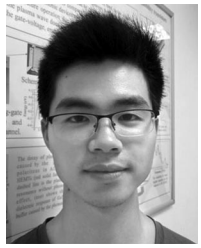

Hehai Fang received the B.S. degree in condensed matter physics from the Nankai University, Tianjin, China, in 2014. He is currently working toward the Ph.D. degree in microelectronics and solid-state electronics at the Shanghai Institute of Technology Physics, Chinese Academy of Sciences, Shanghai, China. His research interests include fabrication and characterization of infrared photodetectors based on low-dimensional materials, including nanowires and two-dimensional materials.

Mingsheng Long received the B.S. degree from Xiangtan University, Xiangtan, China, in 2006, the M.S. degree from South China Normal University, Guangzhou, China, in 2010, and the Ph.D. degree from Nanjing University, Nanjing, China, in 2017.

He is currently a Research Assistant with Prof. Weida Hu's group at the Shanghai Institute of Technical Physics, Chinese Academy of Sciences, Shanghai, China. His research interests include synthesis of novel narrow bandgap layered materials and their infrared physical properties.

Gang Chen received the Ph.D. degree in physics from Fudan University, Shanghai, China, in 2002.

He was a Postdoctoral and Senior Postdoctoral Fellow with the Institute of Semiconductor and Solid Physics, Linz University, Linz, Austria, from 2002 to 2012. He is currently a Professor with the Shanghai Institute of Technology Physics, Chinese Academy of Sciences, Shanghai, China. His research interests include photoelectron applications of germanium silicon quantum dots and nanowires.

Zhe Zheng received the B.S. degree in applied chemistry from Tianjin University, Tianjin, China, in 2014. He is currently working toward the Ph.D. degree in chemistry at Peking University, Beijing, China.

His research interests include carbon nanotube growth and device fabrication.

Jin Zhang received the Ph.D. degree from Lanzhou University, Lanzhou, China, and Peking University, Beijing, China, in 1997.

He is currently a Professor with Peking University. His research interests include chemical vapor deposition growth and chemical synthesis of low dimensional nanomaterials for nanoelectronic devices.

Wenjia Zhou received the B.S. degree in material chemistry from Sichuan University, Chengdu, China, in 2009, and the Ph.D. degree in physics from the Institute of Physics, the Chinese Academy of Sciences, Beijing, China, in 2015, where he worked on fabricating perovskite oxide films and studying their photoelectricity properties.

In 2015, he was with the School of Physical Science and Technology, ShanghaiTech University, as a Postdoctoral Fellow to work. His research interests include solar cells, photodetectors, and other optoelectronic devices from solution-processed semiconductors such as colloidal quantum dots and perovskites.

Zhijun Ning received the Ph.D. degree from the East China University of Science and Technology, Shanghai, China, in 2009.

He is currently an Assistant Professor (Tenure-track) with the School of Physical Science and Technology, ShanghaiTech University, Shanghai, China. His research interests include novel optoelectronic materials including nanocrystals, perovskite, and organic molecules for applications like solar cells, photocatalysis, luminescence, and photodetectors.

Zhihong Zhu received the Ph.D. degree in optical engineering from the National University of Defense Technology, Changsha, China.

His current research interests include fabrication and characterization graphene based optical devices.

Ying Feng received the Ph.D. degree in optical engineering from the National University of Defense Technology, Changsha, China.

Her current research interest include novel optical-electric sensor.

Shiqiao Qin received the Ph.D. degree in optical engineering from the National University of Defense Technology, Changsha, China.

His current research interests include fabrication and characterization graphene based optical devices.

Xiaoshuang Chen received the Ph.D. degree in condensed matter physics from Nanjing University, Nanjing, China, in 1995.

He is currently a Full Professor with the Shanghai Institute of Technology Physics, Chinese Academy of Sciences, Shanghai, China, where he is also the Director of the National Laboratory for Infrared Physics. His current research interests include infrared photo-electronic material design, high-speed electronic device design, and photonic crystal.

Wei Lu received the Ph.D. degree from the Shanghai Institute of Technology Physics, Chinese Academy of Sciences, Shanghai, China, in 1988.

He has been the Research Fellow with the Technical University of Braunschweig, Braunschweig, Germany, since 1989, and a Visiting Professor in many countries. He is currently a Full Professor with the Shanghai Institute of Technology Physics, where he is also the Director.

Weida Hu received the Ph.D. (Hons.) degree in microelectronics and solid-state electronics from the Shanghai Institute of Technology Physics, Chinese Academy of Sciences, Shanghai, China, in 2007.

He is currently a Full Professor with the Shanghai Institute of Technology Physics, Chinese Academy of Sciences. His current research interests include fabrication and characterization of HgCdTe infrared photodetectors, infrared avalanche photodiodes, and low-dimensional (nanowires or two-dimensional materials) infrared photodetectors.